Unraveling the nature of coherent beatings in chlorosomes

Jakub Dostál,[1,2] Tomáš Mančal,[2] František Vácha,[3] Jakub Pšenčík,[2] and Donatas Zigmantas[1,a)]

[1]*Department of Chemical Physics, Lund University, P.O. Box 124, SE-22100 Lund, Sweden*
[2]*Faculty of Mathematics and Physics, Charles University in Prague, Ke Karlovu 3, 121 16 Prague, Czech Republic*
[3]*Faculty of Science, University of South Bohemia, Branišovská 31, 370 05 České Budějovice, Czech Republic*

(Received 27 December 2013; accepted 4 March 2014; published online 20 March 2014)

Coherent two-dimensional (2D) spectroscopy at 80 K was used to study chlorosomes isolated from green sulfur bacterium *Chlorobaculum tepidum*. Two distinct processes in the evolution of the 2D spectrum are observed. The first being exciton diffusion, seen in the change of the spectral shape occurring on a 100-fs timescale, and the second being vibrational coherences, realized through coherent beatings with frequencies of 91 and 145 cm^{-1} that are dephased during the first 1.2 ps. The distribution of the oscillation amplitude in the 2D spectra is independent of the evolution of the 2D spectral shape. This implies that the diffusion energy transfer process does not transfer coherences within the chlorosome. Remarkably, the oscillatory pattern observed in the negative regions of the 2D spectrum (dominated by the excited state absorption) is a mirror image of the oscillations found in the positive part (originating from the stimulated emission and ground state bleach). This observation is surprising since it is expected that coherences in the electronic ground and excited states are generated with the same probability and the latter dephase faster in the presence of fast diffusion. Moreover, the relative amplitude of coherent beatings is rather high compared to non-oscillatory signal despite the reported low values of the Huang-Rhys factors. The origin of these effects is discussed in terms of the vibronic and Herzberg-Teller couplings. © *2014 AIP Publishing LLC*. [http://dx.doi.org/10.1063/1.4868557]

I. INTRODUCTION

In order to efficiently collect incoming sunlight, photosynthetic organisms have developed various types of light-harvesting antennas. These are usually sophisticated pigment-protein complexes, where the properties of the pigment molecules are finely tuned by the encapsulating protein structure. Notable exception to this architecture is represented by chlorosomes—light-harvesting antennas adopted by the species belonging to three phyla of photosynthetic bacteria. While the number of pigments in other photosynthetic antennas usually does not exceed several hundred, the interior of a single chlorosome is composed of a much larger number ($\sim 10^5$) of strongly coupled bacteriochlorophyll (BChl) *c*, *d*, or *e* molecules (depending on species) without any direct interaction with proteins.[1–4] Steady-state and transient absorption spectra of chlorosomes bear a close resemblance to the corresponding spectra of *in vitro* self-assembled BChl aggregates,[5] which proves the dominating contribution of the aggregates to the optical properties of chlorosomes. In addition to BChl molecules as a major constituent, chlorosomes contain a smaller amount of quinone, carotenoid, lipid, and protein molecules. Attached to the chlorosome side, facing cytoplasmic membrane, is the baseplate—a pigment-protein complex containing hundreds of BChl *a* molecules acting as mediators of excitation energy transfer from the chlorosomal body towards the reaction centers.[1,3,4]

Energy transfer within chlorosomes has been studied using femtosecond spectroscopy techniques by several groups, and many different decay components have been identified on the 100 fs to 100 ps time scale depending on the species, growth, and experimental conditions (for review see Refs. 3, 4, and 6). These decays were often observed without a corresponding rise in the spectral region of the excitation acceptor, making it difficult to reliably assign them to energy transfer steps within the chlorosome. One exception is the energy transfer from BChl aggregates to the baseplate, which in *Chlorobi* species containing BChl *c*, such as *Chlorobaculum* (*Cba.*) *tepidum* studied in this work, occurs with the main time constant of 30–40 ps.[4] The second exception is the energy transfer from the blue part of the Q_y absorption band of BChl aggregates to their redshifted states, which was observed in chlorosomes from different species with transfer times between 100 and 1000 fs.[7–10] This process corresponds to exciton relaxation from higher to lower exciton levels. Particularly for *Cba. tepidum* chlorosomes, it is rather fast (100–250 fs),[9] which is perhaps due to their better ordered BChl *c* aggregates as compared to other bacteria species. In addition, our previous two-dimensional (2D) spectroscopy study resolved even a faster, sub-100-fs process, attributed to the exciton diffusion in the highly disordered interior of the chlorosomes.[11] It was proposed that due to a strong disorder in the BChl arrangement the chlorosomal aggregate is effectively broken into smaller parts (coherent domains) that in the first approximation can be viewed as independent systems weakly coupled to each other. The observed ultrafast process corresponds

a)Author to whom correspondence should be addressed. Electronic mail: donatas.zigmantas@chemphys.lu.se

to the energetically downhill-biased diffusion between such neighboring domains.

A typical feature observed in ultrafast experiments is the presence of the short-lived oscillations.[5,12–15] In the case of *Cba. tepidum* two major frequencies of 70–90 cm^{-1} and 130–160 cm^{-1} are usually resolved,[12,15] which approximately coincide with the group of low-frequency modes observed in the resonance Raman scattering data on chlorosomes[16] or artificial thin-solid-film BChl *c* aggregates.[17] The observed oscillations in transient spectra were thus assigned to the coherent beatings between vibrational levels of these modes.[5,12–15] Cherepy *et al.*[16] speculated that these coherences are mostly of excited state origin, however, Ma *et al.*[14] convincingly showed the presence of ground state vibrational coherences by the means of two-color transient absorption measurements on chlorosomes from *Chlorobium phaeobacteroides*, where the Q_y transition was probed after Soret band excitation.

In addition, the resonance Raman study by Bocian and coworkers[17] identified that the same modes are also present in the BChl-related molecules that are incapable of aggregation, but their intensity was very low. Based on this observation it was concluded that these modes belong to the individual pigments and are coupled to the Q_y electronic transition of the supramolecular assembly, which enhances particular resonance Raman transitions. These modes were assigned to out-of-plane deformations of the chlorin macrocycle.

In this work we have studied coherent oscillations in the chlorosomes from *Cba. tepidum* at 80 K using coherent 2D electronic spectroscopy.[18] This method measures third-order polarization response of the sample and provides simultaneous high spectral and temporal resolution. It is thus especially suitable for studying fast photophysical processes in multichromophoric systems, e.g., in photosynthetic complexes. Moreover, 2D spectroscopy provides detailed insight into the quantum coherence phenomenon as has been demonstrated in many studies (see, e.g., Refs. 19–22). We performed the amplitude and phase analysis of the oscillations in two dimensions, which provided us with comprehensive information on coherent beatings and their origin.

II. MATERIALS AND METHODS

Cba. tepidum cells were grown as described previously[23] and the chlorosomes were isolated following the standard method consisting of two successive sucrose gradient ultracentrifugation steps.[24] Before the measurement, the chlorosomes were dissolved in the 2:1 (v/v) mixture of glycerol and 50 mM Tris-HCl buffer (pH 8.0) to achieve absorbance of about 0.35 at 745 nm in a 0.5 mm optical cuvette. We have shown that observed quantum coherences were not dependent on the redox conditions of the sample[25] and therefore in the presented experiments samples were used without addition of any agent controlling the electrochemical potential. All experiments were carried out in a nitrogen continuous flow cryostat (STVP-400, Janis Research Company) kept at a constant temperature of 80 K. Excitation intensity of each laser pulse was set to 100 pJ (photon density of $\sim 4.8 \times 10^{12}$ photons/pulse cm^2).

The detailed description of the experimental setup used to obtain 2D spectra can be found in Refs. 26 and 27. Briefly, the 15 fs long laser pulses centered at 750 nm with FWHM of ~90 nm were generated by the laser system consisting of 200 kHz KGW amplified laser (Pharos, Light Conversion) pumping lab-made non-collinear optical amplifier. The initial beam was split into four parts using a beamsplitter and a transmissive diffraction grating. Pulses were sequenced in time using a conventional optical delay line and inserting fused silica wedges mounted on motorized translation stages. The beams were focused and overlapped in a box-car geometry onto a single spot of the sample. The four-wave mixing signal resulting from the sample interaction with three pumping pulses was emitted into the phase-matching direction. The signal was mixed with the fourth beam (local oscillator), attenuated by an OD 3 filter, and interferometrically detected after transmission through a spectrograph on a CCD camera. Two excitation pulses were modulated at different frequencies by optomechanical choppers. Lock-in detection of the sum and difference chopping frequencies allowed discrimination of the four-wave mixing signal against scattering signals. During the measurements the coherence time (delay between the first two pulses) was scanned in the range from −120 fs to 180 fs with a step of 1 fs, which ensured the resolution of 90 cm^{-1} along the excitation (coherence) frequency axis. The same resolution was achieved along the detection frequency axis, determined by the time domain window used in Fourier analysis.

III. RESULTS AND DISCUSSION

Two distinct processes can be resolved in the time evolution of the real part of the experimental 2D spectrum (Fig. 1(a)). One of them is the exciton diffusion in the highly disordered interior of the chlorosome previously observed in room temperature experiments.[11] This process is manifested by a fast signal amplitude drop during the first 100 fs to approximately half of its initial value (Fig. 2). The decay of the signal is accompanied by the pronounced change of the 2D spectrum shape. Within ~100 fs the diagonally elongated positive part of the 2D spectrum (surrounded at the top and bottom by the negative excited state absorption) extends downwards, completely filling the space under the diagonal. The downhill relaxation part of the diffusion process, which manifests itself as a rounding and shift of the 2D spectrum to the lower detection frequencies, is more distinct at 80 K (Fig. 1) than at room temperature.[11]

Other phenomena, which are well pronounced at low temperature, are coherent beatings damped during the first 1.2 ps (Fig. 2). Note that we have also observed much weaker oscillations in the 2D spectra measured at room temperature.[25] To get a better insight into the properties of the oscillating signals, kinetics at individual points of the 2D spectra were fitted with three decaying exponentials. Residuals after subtraction of multiexponential fits from the kinetic traces together with their Fourier transform amplitudes are shown in Fig. 3. Remarkably, the oscillatory patterns are very similar throughout the whole 2D spectrum and the variations between different regions are limited mainly to the amplitude

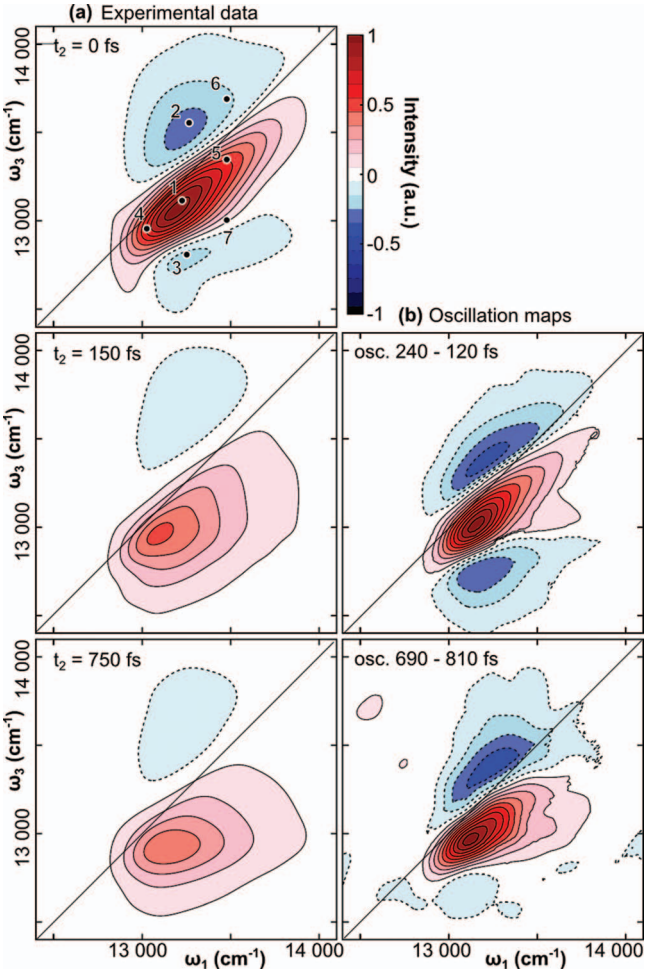

FIG. 1. (a) Time evolution of the 2D spectrum (real part of the electric field). The numbered points indicate the places from where trajectories for further analysis were taken. (b) Time-resolved maps of the distribution of the oscillatory patterns in the 2D spectra, all normalized to their maxima. These maps are obtained by calculating the difference of the oscillatory component from two 2D spectra at indicated population times.

and sign. This similarity allows simple construction of the time-resolved maps demonstrating distribution of the oscillations in the 2D spectra. This is achieved by plotting the signal difference between two consecutive extremes of a large amplitude change observed in all oscillatory patterns at the same population times (see gray regions in Fig. 3). Resulting oscillation distribution maps (Fig. 1(b)) resemble very closely the shape of the 2D spectrum at $t_2 = 0$ fs (correlation spectrum). The relative phase of the oscillations follows the sign of the correlation spectrum, i.e., the oscillations appearing in the 2D spectral regions, where the signal is positive, have the opposite phase to the oscillations appearing in the 2D spectral regions, where the sign is negative. Even though the shape of the 2D spectrum changes substantially during the first 100 fs, the oscillation maps do not follow this change. The oscillating signal evolution in the rephasing and non-rephasing parts is very similar to that of the total signal as described above and is given in the supplemental material.[25]

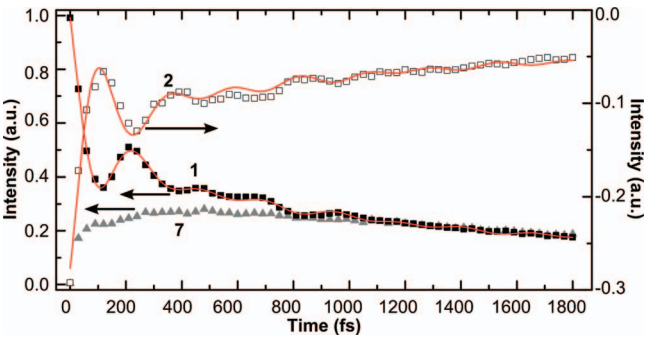

FIG. 2. Time evolution at the selected points in the 2D spectrum. Solid squares correspond to the point in the $t_2 = 0$ fs 2D spectrum with initial signal maximum; open squares—initial signal minimum; gray triangles—initial signal lower nodal line (for the assignment of the numbers to different points in the 2D spectrum see Fig. 1). Lines are the best simultaneous fits by the Eq. (1). Note that the weaker and negative trace 2 has a separate ordinate axis on the right side of the graph.

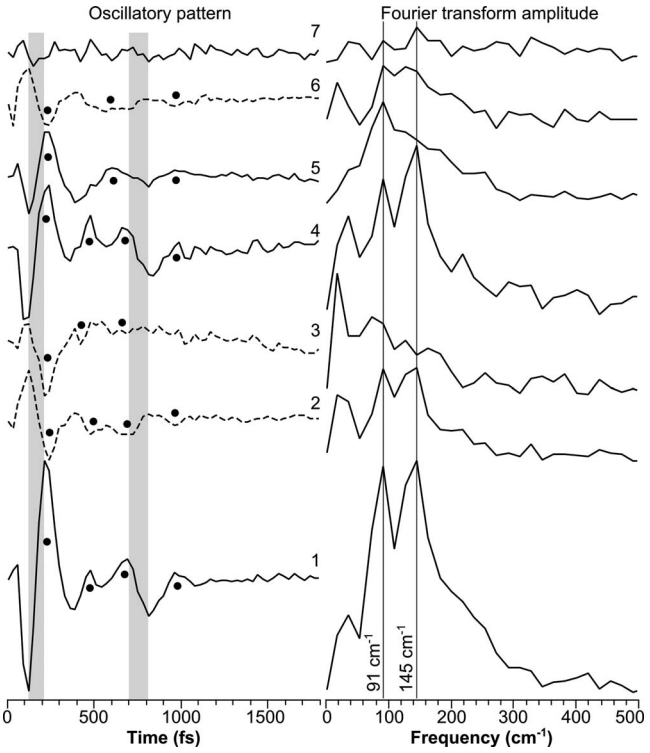

FIG. 3. Oscillatory pattern after subtraction of the three-exponential fit at different points of the 2D spectrum, corresponding to GSB/SE (solid line) or ESA (dotted line) and their Fourier transform amplitude. Numbers assigned to trajectories are introduced in Fig. 1. The black dots mark the main oscillatory features and aid visual reading of the picture. The meaning of the grey regions is explained in the text.

Fourier transform analysis of individual oscillatory traces (Fig. 3) reveals the presence of two main frequencies at ~91 cm^{-1} and ~145 cm^{-1}. Coherent beatings with similar frequencies were observed in the previous investigations of chlorosomes.[12,15] The relative amplitudes of the two modes are very similar, but not completely uniform. The lower-frequency mode tends to dominate in the higher excitation energy side of the spectrum (trajectory 5), whereas the higher-frequency mode prevails in the lower-energy side (trajectory 4). This causes small excitation-frequency-dependent variations in the otherwise very similar oscillatory dynamics. Fourier transformation of the sequences of the 2D spectra residuals in t_2 results in the oscillation maps (Fig. 4). Again, the Fourier amplitude maps of the two dominant frequencies

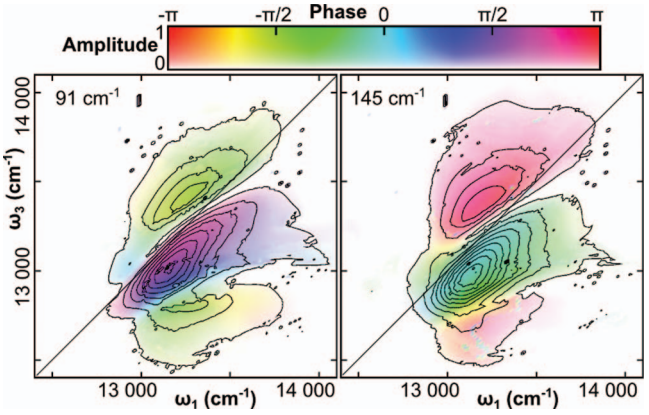

FIG. 4. Amplitude and phase distribution of the individual modes in the 2D spectra obtained from the Fourier transform of the oscillatory part of the data. Contours and the color saturation mark the amplitude, the color hue codes the phase.

at 91 cm^{-1} and 145 cm^{-1} are similar to the elongated shape of the 2D spectrum at $t_2 = 0$ fs. The phase of each mode flips by π between positive and negative regions of the 2D spectrum. Interestingly, these modes do not oscillate in phase, but their relative phases are shifted by approximately $\pi/2$.

A. Origin of the coherent beatings

Since the frequencies of the observed coherent oscillations in the 2D spectra coincide well with the group of lines observed in the resonance Raman experiments (within the resolution of 18 cm^{-1}, given by the t_2 scan),[16,17] the oscillations can be attributed to the coherent vibrational wavepacket motion. For the possible assignment of the modes we follow the detailed work of Czarnecki *et al.*[28] on the reaction centers from purple bacteria containing BChl *a*. Some Raman spectral features in the reaction centers are similar to the features observed in the BChl *c* aggregates.[17] Particularly, the group of modes around 137 cm^{-1} is amplified in the resonance Raman spectrum of a strongly coupled special pair, as compared to the identical modes of weakly coupled accessory BChl *a* pigments. Based on *ab initio* calculation and the isotope labeling, these modes were assigned to the macrocycle doming mode, out-of-plane deformations of the pyrrole rings and in-plane deformation of the acetyl group at C3 (according to the IUPAC nomenclature); all effective at modulating the electronic structure of the dimer. Due to the structural similarity between BChl *c* and *a* molecule the qualitatively similar modes could be responsible for the 145 cm^{-1} mode observed in chlorosomes. Obviously, vibration of the acetyl group at C3 does not contribute because this group is replaced by the 1-hydroxyethyl group in BChl *c*. The modes with frequencies similar to 90 cm^{-1} were also observed in the reaction centers, but their intensity was weak. These modes were assigned to the out-of-plane deformations of peripheral groups, most notably the methyl group at $C3^1$ and keto oxygen at $C13^1$. Both groups (the former being part of the hydroxyethyl group at C3 in the BChl *c* molecule) are essential for formation of the BChl *c* aggregates.[29] It is reasonable to assume that their vibrations affect the interaction strength between excitonically coupled BChl *c* pigments, thus making them sensitive to the electronic state changes and therefore being enhanced in the resonance Raman scattering.

Vibrational coherence oscillations in the 2D spectra occur due to the three types of contributions to the transient signal: ground state bleaching (GSB), stimulated emission (SE), and excited state absorption (ESA). Oscillations with different phase can appear in all parts of the spectrum when vibrational quantum energy is comparable to the extent of the 2D spectrum.[30,31] Note that in the case of chlorosomes, vibrational quanta of the modes (∼91 cm^{-1} and ∼145 cm^{-1}) are much smaller than the ω_3 difference between the positive and negative parts in the 2D spectra (points 1 and 2 in Fig. 1), which is approximately 500 cm^{-1}. This leads to the conclusion that the beatings in the regions where the oscillation phase is opposite to the phase at the maximum of the positive signal should originate from ESA. This is also supported by almost identical shapes of the negative regions in the correlation 2D spectrum and oscillation distribution maps. It implies that the part of the oscillations that are simultaneously observed in the positive region as oscillatory SE and in the negative region as oscillatory ESA come from the vibrational wavepacket dynamics in the excited electronic states. On the other hand, vibrational coherences in the ground state (previously documented in Ref. 14) manifested as oscillatory GSB should be located in the region of positive signal.

The ratio between the excited and ground state contributions to the oscillatory signals is not completely clear. The basic theoretical considerations of an electronic system with vibrational progression predict an equal intensity of coherences from the ground and excited states due to the (anti)symmetry of Franck-Condon factors. Excited and ground state contributions should in principle differ in their dephasing times in the presence of the fast energy relaxation to the ground state (possibly connected with the Förster energy transfer to a neighboring molecule), during which the excited state coherence disappears completely, while the one in the ground state may dephase only partially.[32] From Fig. 2 it is apparent that the oscillatory ESA is almost a perfect mirror image of the oscillations obtained from the central part of the positive signal. One of two possible implications is that the fast diffusion process is either capable of dephasing the ground and excited state coherences on the same timescale, making both types indistinguishable even on the basis of their dynamic properties. The other implication could be that the excited state coherences are much stronger making the ground state coherences observable only in the specially designed experiments, such as two-color transient absorption measured with relatively long laser pulses.[14]

Another notable observation is that the amplitude of coherences is relatively high compared to the intensity of the exponentially decaying non-oscillatory part of the signal. This could indicate a rather high value of the Huang-Rhys (HR) factors. However, the values of the HR factor of the low frequency modes in the chlorosomes from *Chloroflexus aurantiacus* have been estimated to lie in the range of 10^{-2} by simultaneous fitting of the linear absorption and the resonance Raman spectra.[16] The absolute intensities of the resonance Raman lines of the chlorosomes from *Cba. tepidum*

reported in the same work are lower, indicating even lower values of the HR factors. Moreover, only the modes around 50–170 cm^{-1} are observed as coherent beatings in the femtosecond experiments, whereas the other modes of comparable and even higher intensities in the resonance Raman experiments are not observed in time-resolved studies.[12,14,15] In contrast to the chlorosome data reported by Cherepy *et al.*,[15] the resonance Raman spectra of the BChl *c* thin-solid-film aggregates[17] are dominated by two distinctive peaks at frequencies of ∼115 cm^{-1} and ∼145 cm^{-1}. These modes represent a close match to the Fourier transforms frequencies of the oscillatory components observed in the ultrafast experiments. This correspondence suggests that the HR factor of these modes in chlorosomes could be rather high. The discrepancy between the resonance Raman spectra of chlorosomes and BChl *c* aggregates is quite striking, since many other spectroscopic properties (including coherent beatings) are almost identical for these two systems.[5] In addition, the correspondence between enhanced low-frequency resonance Raman modes and strong coherent beatings with the same frequencies have been previously reported for porphyrin J-aggregates.[33] From all the mentioned cases it can be implied that the enhancement of the low frequency modes is quite a general phenomenon in large aggregates of porphyrin based molecules.

To explain why only certain low-frequency modes are enhanced in the chlorosome experiments we provide a couple of interpretations. One possible explanation could be the enhancement of the vibrational coherences by the intensity borrowing from the resonant electronic transition. Such enhancement mechanisms have been recently explored in idealized dimer systems,[34–36] and we can speculate that in the case of more complicated systems such as chlorosomes the induced effects can grow in complexity, possibly causing the contribution of the excited state coherences to enhance disproportionally. The advantage of this interpretation is that the mechanism does not require a big HR factor. The necessary resonant electronic transition can be readily present in the single exciton manifold due to the complex coupling between the molecules in the three-dimensional aggregate. On the other hand, a strong and disproportional enhancement of only the excited state part of the oscillations cannot be inferred from the current theoretical models.

Another option would be to consider theoretical models which go beyond the Franck-Condon approximation. The Herzberg-Teller coupling of the nuclear vibrations to the electronic transition has been previously used by Kano *et al.*[33] to explain very similar observations of coherences in porphyrin J-aggregates. Here we show that strong coupling of the Herzberg-Teller (HT) active low-frequency mode leads to an increase of their HR factor. The effect is demonstrated in an excitonically coupled homodimer of molecules with the Huang-Rhys factors equal to zero. Let us assume that the strength of the transition dipole moments μ of the molecules weakly depends on the vibrational coordinate q of some particular mode (Herzberg-Teller effect):[37,38]

$$\mu = \mu_0\left(1 + \xi\frac{q}{q_0}\right), \tag{1}$$

where the small dimensionless parameter ξ characterizes the strength of the HT effect, μ_0 is the transition dipole moment in the Condon approximation, and q_0 provides the unit of vibrational coordinate. Standard representation of q_0 is given by

$$q_0 = \sqrt{\frac{2\hbar}{m\omega}}, \tag{2}$$

where m stands for the effective mass of the oscillator with the angular frequency ω. Due to the dipole moment dependence on the vibrational coordinate, coupling between molecules J becomes dependent on the vibrational coordinate as well. For simplicity assume dipole-dipole coupling

$$\begin{aligned} J &= \mu(q_1)\mu(q_2)\frac{\kappa}{r^3} = \mu_0^2\frac{\kappa}{r^3}\left(1 + \frac{\xi}{q_0}(q_1+q_2) + \frac{\xi^2}{q_0^2}q_1q_2\right) \\ &= J_0\left(1 + \frac{\sqrt{2}\xi}{q_0}q_+ + \frac{\xi^2}{2q_0^2}\left(q_+^2 - q_-^2\right)\right), \end{aligned} \tag{3}$$

where the subscripts 1 and 2 index individual molecules, κ stands for the orientational factor, r - for the distance between the molecules, and J_0 - for the the dipole-dipole coupling in the Condon approximation. In the last equality we used the basis transformation $q_\pm = 2^{-1/2}(q_1 \pm q_2)$ into the collective symmetric (+) and antisymmetric (−) vibrational coordinates that represent the synchronized in-phase and off-phase vibrations of both molecules, respectively.

The exciton coupling between the molecules leads to the splitting of the single exciton levels $E_\pm = E_0 \pm J(q_+,q_-)$.[39] Evolution of the symmetric mode on the $E_\pm$ potential energetic surface is thus governed by the Hamiltonian (neglecting all small terms quadratic in ξ):

$$\begin{aligned} H_{vib} &= \frac{p_+^2}{2m} + \hbar\omega\frac{q_+^2}{q_0^2} \pm J_0\frac{\sqrt{2}\xi}{q_0}q_+ \\ &\approx \frac{p_+^2}{2m} + \hbar\omega\left(\frac{q_+}{q_0} \pm \frac{\xi J_0}{\sqrt{2}\hbar\omega}\right)^2, \end{aligned} \tag{4}$$

which corresponds to the Hamiltonian of the harmonic oscillator displaced by the HR factor

$$S = \frac{1}{2}\left(\frac{\xi J_0}{\hbar\omega}\right)^2. \tag{5}$$

Thus, although we assumed that the HR factor of each molecule is equal to zero, the collective delocalized symmetric oscillation in the dimer gains the non-zero HR factor by the HT coupling. Consequently, vibrational coherences of the HT mode in electronic ground and excited sates of the dimer can be excited. From Eq. (5) follows that the HR factor enhancement effect is strong only for the low-frequency modes of strongly coupled molecules that have some HT activity. These requirements are well in line with what has been observed in chlorosomes.

The derivation is valid for the large aggregate (like chlorosome) as well with an exception that the energy level splitting approaches $4J$ instead of $2J$ and all the formulas would have to be modified accordingly. If we plug the typical values for chlorosome ($2J_0 \approx 1200\ cm^{-1}$, $\hbar\omega \approx 100\ cm^{-1}$) in

(5), we obtain reasonably high value for the HR factor of 0.18 even for the small HT coupling parameter $\xi = 0.05$.

The proposed HT mechanism explains the selective enhancement of the low-frequency modes in chlorosomes and in other big aggregates.[33] However, it does not provide a mechanism that could either dephase both the excited and ground state coherences on the same timescale or substantially diminish the ground state coherence.

B. Dephasing of the coherences by the diffusion process

The common description of the transfer process between weakly coupled domains, formulated in terms of (multichromophoric) Förster rates, assumes an exponential damping of the donor signal, while the ESA, SE, and GSB of the acceptor exponentially rise. In principle, excited state vibrational coherences could be transferred between the electronic states in the chlorosomes because vibrational oscillation periods (220–370 fs) are longer than the typical transfer time observed in the diffusion processes (∼100 fs).[11] However, the observation that the oscillation amplitude map copies the initial shape of the 2D spectrum implies that the random energy diffusion process is not capable of transferring coherences between different coherent domains. In our previous work[32] we used the theory developed in Ref. 40 to show that a single step of energy transfer leads (for the oscillation frequency 150 cm^{-1} and depopulation rate 1/100 fs^{-1}) to a 70% loss of the amplitude of the oscillations. Since during the diffusion-like energy transfer in chlorosomes such a transfer step is rapidly followed by further steps, it leads us to a conclusion that the transfer of the coherent nuclear oscillations between excited states of the molecules should not be observable.

We conclude that the initially excited domains can be the only source of the oscillatory signals in the 2D spectra of the chlorosomes. The vibrational coherences in the domains are quickly attenuated with the diffusion time of $\tau_1 \sim 100$ fs. We denote the probability that the vibrational coherence is created in the domain that quickly diffuse energy by p. A small fraction of domains $(1 - p)$ that do not undergo diffusion keep beating, and they are dephased on a slower time scale. The value for the slower dephasing time $\tau_2 = 1$ ps was estimated from the fitting procedure described below and it is in agreement with the time component observed previously in several studies.[5,12,13,15,41] The origin of this component is widely discussed and is generally attributed to the slower energy transfer processes in chlorosomes. Two characteristic oscillating traces, corresponding to the maximum positive and maximum negative 2D signals (and having the highest oscillation amplitudes) that are presented in Fig. 2, were simultaneously fitted with the model that describes the main observed features:

$$I(t) = \left[p\mathrm{e}^{\frac{-t}{\tau_1}} + (1-p)\mathrm{e}^{\frac{-t}{\tau_2}}\right]\left[A_1 \cos\left(\omega_1 t + \frac{\pi}{2}\right) + A_2 \cos(\omega_2 t)\right] + B_1\mathrm{e}^{\frac{-t}{\tau_1}} + B_2\mathrm{e}^{\frac{-t}{\tau_2}} + C. \quad (6)$$

The two main oscillating modes have frequencies $\omega_{1,2}$ (92 cm^{-1} and 142 cm^{-1}) and their phases are shifted by $\pi/2$ from each other. Both oscillations are dephased by a pair of independent processes with time constants $\tau_{1,2}$. The same time constants describe the two-exponential decay of the signal intensity, consistently binding together diffusion and dephasing processes. The corresponding fitted curves are plotted in Fig. 2. The fitting parameters are summarized in Table I showing that the fraction $(1 - p)$ of the domains that do not dephase during the 100-fs diffusion is of the order of a few percent.

TABLE I. Set of parameters of model (1) that best simultaneously fit the evolution of the 2D spectrum maximum and minimum (traces 1 and 2).

τ_1 (fs)	τ_2 (fs)	ω_1 (cm^{-1})	ω_2 (cm^{-1})	p
101	1031	92	142	0.93

IV. CONCLUSIONS

We report a low temperature coherent 2D spectroscopy study of the chlorosomes from bacterium *Cba. tepidum*. The observations are consistent with the theoretical model previously presented in Ref. 11, describing the chlorosomes as light harvesters composed of weakly coupled domains mutually exchanging the energy by a random ultrafast diffusion process. In addition to this distinctive process manifested by the pronounced evolution of the 2D spectrum shape, the quantum beatings caused by the coherent vibrational wavepacket motion is resolved at 80 K. Remarkably, some of the beatings are able to significantly outlive the diffusion process, being observable as long as 1.2 ps. However, distribution of the oscillation amplitudes during their entire lifetime persistently copies the initial shape of the 2D spectrum, which identifies their origin in a fraction of domains unaffected by the diffusion. This also demonstrates that the diffusion process is not capable of transferring vibrational coherences between the domains. In addition we discuss interpretation of the high relative amplitude of the coherent beatings and the uniformity of the dephasing rates across the whole 2D spectrum.

ACKNOWLEDGMENTS

The work in Lund was supported by the Swedish Research Council and the Knut and Alice Wallenberg Foundation. The work in the Czech Republic was supported by the Czech Science Foundation (projects P501/12/G055 and P205/10/0989).

[1] N.-U. Frigaard and D. A. Bryant, in *Complex Intracellular Structures in Prokaryotes*, edited by J. Shively (Springer, Berlin, 2006), pp. 79–114.
[2] D. A. Bryant, A. M. G. Costas, J. A. Maresca, A. G. M. Chew, C. G. Klatt, M. M. Bateson, L. J. Tallon, J. Hostetler, W. C. Nelson, J. F. Heidelberg, and D. M. Ward, Science **317**, 523 (2007).
[3] R. E. Blankenship and K. Matsuura, in *Light-Harvesting Antennas in Photosynthesis*, edited by B. R. Green and W. W. Parson (Kluwer Academic Publishers, Dordrecht, 2003), pp. 195–217.
[4] R. E. Blankenship, J. M. Olson, and M. Miller, in *Anoxygenic Photosynthetic Bacteria*, edited by R. Blankenship, M. Madigan, and C. Bauer (Springer Netherlands, 1995), pp. 399–435.
[5] S. Savikhin, P. I. van Noort, R. E. Blankenship, and W. S. Struve, Biophys. J. **69**, 1100 (1995).

[6]G. T. Oostergetel, H. van Amerongen, and E. J. Boekema, Photosynth. Res. **104**, 245 (2010).
[7]S. Savikhin, Y. Zhu, R. E. Blankenship, and W. S. Struve, J. Phys. Chem. **100**, 17978 (1996).
[8]J. Martiskainen, J. Linnanto, R. Kananavičius, V. Lehtovuori, and J. Korppi-Tommola, Chem. Phys. Lett. **477**, 216 (2009).
[9]J. Martiskainen, J. Linnanto, V. Aumanen, P. Myllyperkiö, and J. Korppi-Tommola, Photochem. Photobiol. **88**, 675 (2012).
[10]J. Pšenčík, Y.-Z. Ma, J. B. Arellano, J. Hála, and T. Gillbro, Biophys. J. **84**, 1161 (2003).
[11]J. Dostál, T. Mančal, R. Augulis, F. Vácha, J. Pšenčík, and D. Zigmantas, J. Am. Chem. Soc. **134**, 11611 (2012).
[12]S. Savikhin, P. I. van Noort, Y. Zhu, S. Lin, R. E. Blankenship, and W. S. Struve, Chem. Phys. **194**, 245 (1995).
[13]S. Savikhin, Y. Zhu, S. Lin, R. E. Blankenship, and W. S. Struve, J. Phys. Chem. **98**, 10322 (1994).
[14]Y.-Z. Ma, J. Aschenbrücker, M. Miller, and T. Gillbro, Chem. Phys. Lett. **300**, 465 (1999).
[15]V. I. Prokhorenko, D. B. Steensgaard, and A. R. Holzwarth, Biophys. J. **79**, 2105 (2000).
[16]N. J. Cherepy, M. Du, A. R. Holzwarth, and R. A. Mathies, J. Phys. Chem. **100**, 4662 (1996).
[17]J. R. Diers, Y. Zhu, R. E. Blankenship, and D. F. Bocian, J. Phys. Chem. **100**, 8573 (1996).
[18]D. M. Jonas, Annu. Rev. Phys. Chem. **54**, 425 (2003).
[19]G. S. Engel, T. R. Calhoun, E. L. Read, T.-K. Ahn, T. Mančal, Y.-C. Cheng, R. E. Blankenship, and G. R. Fleming, Nature (London) **446**, 782 (2007).
[20]A. Nemeth, F. Milota, T. Mančal, V. Lukeš, H. F. Kauffmann, and J. Sperling, Chem. Phys. Lett. **459**, 94 (2008).
[21]D. B. Turner, K. E. Wilk, P. M. G. Curmi, and G. D. Scholes, J. Phys. Chem. Lett. **2**, 1904 (2011).
[22]S. Westenhoff, D. Paleček, P. Edlund, P. Smith, and D. Zigmantas, J. Am. Chem. Soc. **134**, 16484 (2012).
[23]J. Pšenčík, T. P. Ikonen, P. Laurinmäki, M. C. Merckel, S. J. Butcher, R. E. Serimaa, and R. Tuma, Biophys. J. **87**, 1165 (2004).
[24]D. B. Steensgaard, K. Matsuura, R. P. Cox, and M. Miller, Photochem. Photobiol. **65**, 129 (1997).
[25]See supplementary material at http://dx.doi.org/10.1063/1.4868557 for data measured at room temperature and anaerobic conditions and for oscillation distribution in rephasing and non-rephasing parts of the 2D spectrum.
[26]R. Augulis and D. Zigmantas, Opt. Express **19**, 13126 (2011).
[27]R. Augulis and D. Zigmantas, J. Opt. Soc. Am. B **30**, 1770 (2013).
[28]K. Czarnecki, J. R. Diers, V. Chynwat, J. P. Erikson, H. A. Frank, and D. F. Bocian, J. Am. Chem. Soc. **119**, 415 (1997).
[29]T. S. Balaban, H. Tamiaki, and A. R. Holzwarth, Top. Curr. Chem. **258**, 1 (2005).
[30]T. Mančal, N. Christensson, V. Lukeš, F. Milota, O. Bixner, H. F. Kauffmann, and J. Hauer, J. Phys. Chem. Lett. **3**, 1497 (2012).
[31]V. Butkus, D. Zigmantas, L. Valkunas, and D. Abramavicius, Chem. Phys. Lett. **545**, 40 (2012).
[32]T. Mančal, J. Dostál, J. Pšenčík, and D. Zigmantas, Can. J. Chem. **92**, 135 (2014).
[33]H. Kano, T. Saito, and T. Kobayashi, J. Phys. Chem. A **106**, 3445 (2002).
[34]N. Christensson, H. F. Kauffmann, T. Pullerits, and T. Mančal, J. Phys. Chem. B **116**, 7449 (2012).
[35]A. Chenu, N. Christensson, H. F. Kauffmann, and T. Mančal, Sci. Rep. **3**, 2029 (2013).
[36]V. Tiwari, W. K. Peters, and D. M. Jonas, Proc. Natl. Acad. Sci. U.S.A. **110**, 1203 (2013).
[37]G. Herzberg and E. Teller, Z. Phys. Chem. **21**, 410 (1933).
[38]G. Orlandi and W. Siebrand, J. Chem. Phys. **58**, 4513 (1973).
[39]M. Kasha, H. Rawls, and M. Ashraf El-Bayoumi, Pure Appl. Chem. **11**, 371 (1965).
[40]M. Yang and G. R. Fleming, J. Chem. Phys. **111**, 27 (1999).
[41]J. Pšenčík, T. Polívka, P. Němec, J. Dian, J. Kudrna, P. Malý, and J. Hála, J. Phys. Chem. A **102**, 4392 (1998).